Synthesis of crosslinked PVA-ceramic composite membrane for phenol removal from aqueous solution

VANDANA GUPTA and JAYAPAL ANANDKUMAR*

Department of Chemical Engineering, National Institute of Technology Raipur, Chhattisgarh-490210, India

Abstract: In this study, the thin-film composite membrane (TFCM) was fabricated for phenol–water separation using formaldehyde crosslinked polyvinyl-alcohol (PVA) coating on fly ash-fuller clay ceramic substrate. Thin film was created using 10 % PVA with different concentrations of formaldehyde (1–5 g). The characterization of synthesized membrane such as swelling and chemical stability, permeation study, molecular weight cut off (MWCO), scanning electron microscopy (SEM) and contact angle analysis was carried out to optimize the membrane. The stability of active layer increases with increase in the amount of formaldehyde, whereas the hydrophilicity, degree of swelling, flux and pore size decrease. The smallest pore (1.91 nm) was obtained in the active layer when PVA crosslinked with 3 g formaldehyde (PF$_3$). Phenol–water separation was conducted with PF$_3$ to optimize the process parameters, such as feed concentration, pH and operating pressure. Maximum phenol separation (85 %) was obtained at 207 kPa for 200 mg L^{-1} of feed phenol. High phenol removal was found at pH 6.0 and thereafter it decreased in alkaline pH. Phenol removal decreased from 80.6 to 19.8 % with the increase in pressure from 207 to 414 kPa, whereas flux increased from 5.3 to 52.38 L m^{-2} h^{-1}. The results demonstrate that fabricated CM can be successfully used for phenol–water separation.

Keywords: phenol removal; composite membrane; fuller clay; PVA; fly ash.

INTRODUCTION

Wastewater discharged from many industries such as pesticide, petrochemical, pharmaceutical printing, *etc.*, contains various toxic organic pollutants which are carcinogenic to human beings as well as to flora and fauna.[1,2] These organic pollutants include benzene and its derivative phenol which cause high risk both to human and ecological system. Therefore, these toxic organic pollutants must be treated before they are discharged in to the environment. Many conventional

techniques are used for phenol removal from wastewater and each technique has some disadvantages such as high cost, low efficiency, high energy consumption and difficulties in recycling.[3] Removal of phenol from aqueous solution by pervaporation is widely used, but pervaporation is an energy intensive process.[3–5] In recent days, the phenol removal by ultrafiltration, microfiltration, nanofiltration and reverse osmosis membrane filtration became more demanded techniques for good phenol removal efficiency.[3,6–11]

Nowadays, composite membranes (CM) are gaining more attention for many applications due to its remarkable properties. Recently, thin film composite membranes (TFCM) have been reported to possess superior structural integrity, flux, resistance to fouling and high selectivity.[12–14] However, their utility in industry is not widely spread due to the high fabrication cost of CM. The cost of composite membrane is three to four times higher than that of the thin film polymeric membrane, owing to the high cost of its support alone.[12] Hence, there is a necessity to look for the alternative in expensive resources and methods for fabrication of support, in order to produce the commercially applicable CM. Among the several available membrane supports, the ceramic supports are attractive due to their high mechanical strength, chemical and temperature resistivity. Inexpensive ceramic supports can be prepared of waste fly ash, locally available clay, kaolin *etc.*[12,14–16] The matter of interest in this study is the preparation of an inexpensive polymeric TFCM and the enhancement of its industrial applicability. TFCM consists of top thin polymeric layer as active membrane surface, coated on a substrate. The substrate is prepared using locally and abundantly available low-cost coal fly ash, which consists of Al_2O_3, SiO_2 and Fe_2O_3. These constituents enhance the porosity, chemical stability and mechanical strength of the substrate.[15] Wide range of polymeric materials, which can be used as active top layer of composite membrane, is available. Some researchers have reported the synthesis of CM using polyvinyl alcohol, cellulose acetate, polydimethylsiloxane, polysulfone, *etc.*, coated on different substrate (polymeric, ceramic, carbon nanotube, *etc.*) with good separation efficiency.[12–14,17–20]

Polyvinyl alcohol (PVA) has been chosen as polymeric material for the active top layer in the present study. PVA has excellent hydrophilic nature and hence it is widely used in pervaporation process for the removal of small fractions of water from organic solution.[21] However, the hydrophilic nature of PVA restricts its direct usage with aqueous solutions. The properties of PVA can be modified by crosslinking with a suitable crosslinking agent. Crosslinking agents can modify the PVA properties such as tensile strength, elasticity, impact strength, solubility and diffusivity, which are attributed to the presence of abundant hydroxyl groups (–OH) in polymer chain.[21,22] The crosslinking of PVA by different crosslinking agents has been reported in the literature,[23,24] stating that glutaraldehyde, maleic acid, aluminium acetylacetonate and formaldehyde are

widely used.[3,21,25–29] The use of formaldehyde as a crosslinking agent for PVA membrane exhibited particularly good results.[29,30] The PVA membrane modified by crosslinking is proved to be suitable for various applications such as rejection of organic compounds, microbial fuel cell, protein rejection, *etc.*[13,27,32]

In this study, TFCM was synthesized using crosslinked PVA active layer coated on ceramic substrate by simple glass rod coating technique. The amount of crosslinking agent (formaldehyde) was optimized to get a best suited PVA layer for phenol–water separation. The properties of TFCM were characterized in terms of morphology, permeation, water uptake, molecular weight cut-off and pore size. The phenol–water separation efficiency by synthesized TFCM was tested using various operating parameter such as applied pressure, feed pH and concentration.

MATERIALS AND METHODS

Materials

Polyvinyl alcohol (Molecular wt: 115000, degree of hydrolysis 98–99 %), formaldehyde (37–40 %), kaolin, boric acid, sodium metasilicate, sodium carbonate, potassium ferricyanide, phosphate buffer and poly(ethylene glycol) (molecular weight: 1500, 4000, 6000, 10,000 and 20,000) were procured from Loba Chemie Pvt. Ltd., India. Phenol, ammonia solution (25 %) and 4-aminoantipyrene were purchased from Merck India Pvt. Ltd. Fuller clay was procured from local supplier and double distilled water was used as solvent. Fly ash was collected from National thermal power corporation, Korba, India.

Fabrication of composite membrane

Initially, the ceramic support was prepared by mixing different constituents at certain proportion using uniaxial method (Table I). Afterwards, various CMs were prepared using PVA (10 wt. %) solution crosslinked with six different amounts of formaldehyde. These CMs are named as PF_0, PF_1, PF_2, PF_3, PF_4 and PF_5 for 0, 1, 2, 3, 4 and 5 g formaldehyde with PVA solution, respectively. Detailed methodology for CM synthesis is given in the Supplementary material to this paper.

TABLE I. Composition of ceramic support

Components	Fly ash	Fuller clay	Kaolin	Boric acid	Sodium metasilicate	Sodium carbonate
Amount, wt. %	72	8	15	1.25	1.25	2.5

Membrane characterization

Swelling and chemical stability test. Water uptake capacity of ceramic support and CM was performed in terms of the swelling degree. The experiment was carried out by immersing membrane in distilled water for 48 h. Then sample was taken out, wiped gently using tissue paper to remove excess water, and weighed immediately. The swelling degree of polymeric active layer (Sd_a) can be calculated by the following equation:

$$Sd_a = 100\left(\frac{W_{cw} - W_{cd}}{W_{cd}} - S_w \right)$$

(1)

where, W_{cd} and W_{cw} are the dry and wet mass of CM and S_w is the swelling degree of support in distilled water.

Swelling degree (Sd) of support can be calculated as follows:[17,19,27]

$$Sd = 100\frac{W_w - W_d}{W_d} \tag{2}$$

where W_d and W_w are the dry and wet mass of membrane.

Chemical stability of CM was examined by immersing the membranes in a highly acidic (pH 2) and highly alkaline (pH 12) media. Chemical stability of the membranes was tested for the period of one week. The samples were dried and mass loss was calculated. The amount of mass loss is related to the stability of active top layer in harsh chemical environment.

Permeation study and pore size determination. Compaction and permeation study was carried out using dead-end filtration setup to examine the water transport property through CM. The schematic diagram of dead-end filtration setup is shown in Fig. S-1 (Supplementary material to this paper). Filtration setup consists of 250 ml stainless steel tubular cell with a flat circular base plate. CM was fixed at the centre of the bottom plate. Compaction study was conducted by filling the the tubular cell with distilled water and pressurized at 345 kPa for 4 h. Water flux was calculated for every 10 min interval till the steady state condition was reached. After the compaction study, CM was subjected to pure water permeation test with different pressures (68.94–275.79 kPa). Pure water flux (J) and porosity (ε) were calculated by using the following expressions:

$$J = \frac{q}{At} \tag{3}$$

$$\varepsilon = \frac{W_{wa} - W_{da}}{\rho V} \tag{4}$$

where q, A and t are the volume, L, of permeate, effective area, m², of CM and time, h, for permeation, respectively. W_{wa}, W_{da}, ρ and V are wet mass of active layer, dry mass of active layer, density of water and volume displaced by active layer, respectively.

Molecular weight cut off (*MWCO*) study was conducted with different molecular weights of polyethylene glycol (PEG) to find the pore size of the synthesized CM. In this study, the set of permeation experiment was conducted using 1.5, 4, 6, 10 and 20 kDa molecular weights of PEG. PEG feed solution of 10 kg m⁻³ was prepared with ion free water and allowed to permeate through the CM at constant pressure of 276 kPa.[32,33] PEG concentration in permeate was measured by Abbe refractometer (model 135005, Contech, India). Rejection (R / %) and it was determined by following equation:

$$R\,/\,\% = 1 - \frac{100C_p}{C_f} \tag{5}$$

where C_f and C_p are feed and permeate concentration, respectively.

Average pore radius of membrane can be calculated by Guerout–Elford–Ferry relation:

$$r_m = 16.73 \times 10^{-10} M_w^{0.557} \tag{6}$$

where r_m and M_w is the pore radius (cm) and molecular weight cut off of membrane (Da), respectively.

SEM and contact angle analysis. Morphological structure of different crosslinked active layer and support was examined by the scanning electron microscopy (SEM, model EV018,

Carl Zeiss, Germany). The effect of cross-linking agent on hydrophilic nature of active layer was determined by contact angle analyser (model Phoenix 300, SEO, Korea) using the sessile drop method. Double distilled water was dropped on top of the active layer at 6 different sites and the average value of contact angle between water droplet and active layer was measured.

Removal of phenol from phenol/water binary system

Phenol separation experiments were carried out with all CM. Operating parameters such as suitable CM, feed concentration (50–200 mg/l), operating pressure (68–414 kPa) and feed pH (2–12) were optimized in order to get high separation efficiency. Permeate was collected at a regular time interval and flux through CM was calculated by equation 3. Feed and permeate phenol concentration was determined by 4-aminoantipyrene method (APHA, 2012).[34] Phenol rejection was calculated by Eq. (5).

RESULT AND DISCUSSION

Characterization of membrane

Swelling and chemical stability test. The degree of swelling in terms of water uptake capacity of membrane was calculated by Eq. (1). Fig. 1a shows the
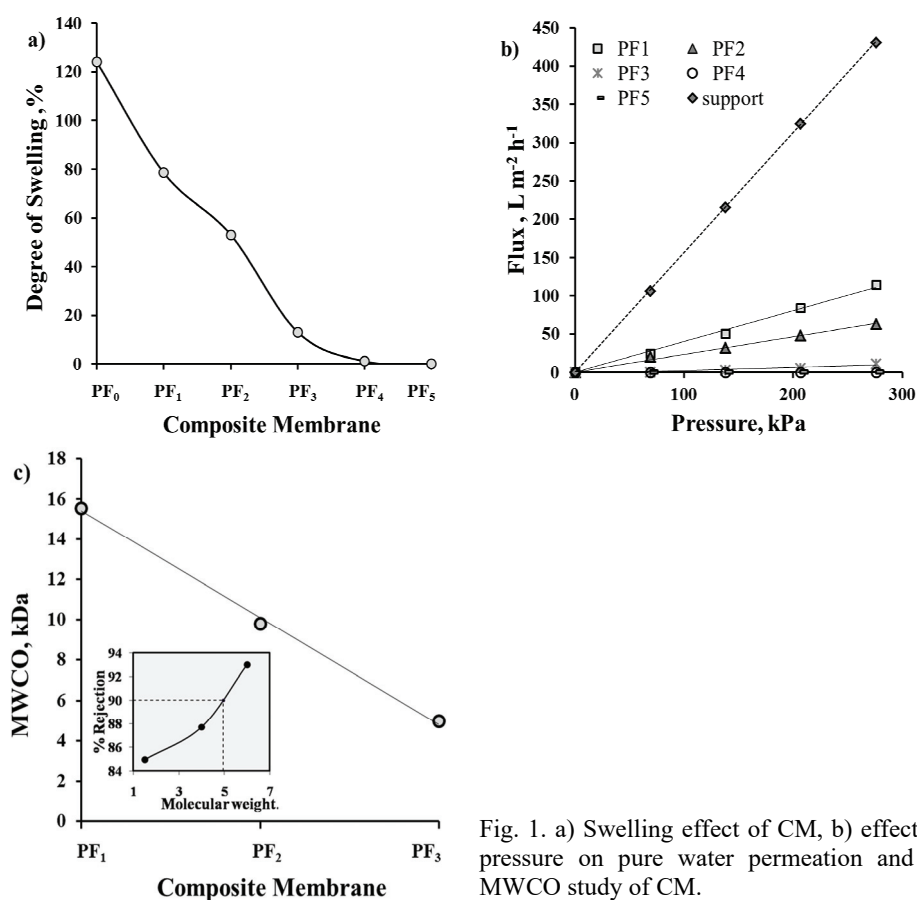

Fig. 1. a) Swelling effect of CM, b) effect of pressure on pure water permeation and c) MWCO study of CM.

decrease of swelling with increase in formaldehyde incorporation (from PF_0 to PF_5). The decrease in swelling is due to the formation of acetal ring. Acetal ring linkage over the outermost surface of the membrane decreases the hydrophilic nature of membrane, therefore swelling reduces.[27] The increase in the amount of formaldehyde caused symmetrical channels orientation within the membrane, which gives a high mechanical strength by reducing the water holding capacity of membrane.[27] The chemical stability of the different CMs (PF_1–PF_5) was carried out at highly acidic and alkaline condition. The results of the chemical stability test are given in Table II. There was negligible change in the mass loss when PF_1–PF_5 were immersed in the highly alkaline (pH 12) and highly acidic (pH 2) media. However the active layer of PF_0 was instable in both media. The loss of stability is due the highly hydrophilic nature and to the swelling of pure PVA (PF_0). The increase in formaldehyde amount caused the decrease in hydrophilic nature of the active layer hence the stability of active layer increases and proves its suitability for harsh chemical environment.

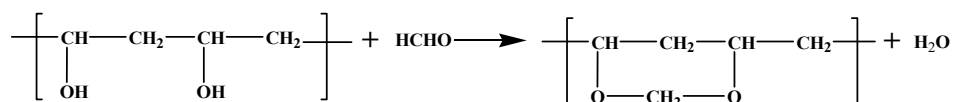TABLE II. Physiochemical properties of composite membrane

Parameter		Support	PF_0	PF_1	PF_2	PF_3	PF_4	PF_5
Average pore size, nm		14	14	3.6	2.8	1.9	–	–
Active layer thickness, mm		–	0.8	0.8	0.8	0.8	0.8	0.8
Pure water flux, L m^{-2} h^{-1}		325	202.4	84.4	48	5.6	0	0
Contact angle, °		–	32.4	39.5	46.9	52	57.1	63.9
Chemical stability	pH 2	–	Not stable	1.1	1.2	1.5	1.6	1.7
(weight loss, %)	pH 12	–	Not stable	0.18	0.11	0.35	0.06	0.06

Permeability and pore characteristics of CM. The compacted support and CM was subjected to pure water permeation. Hydraulic permeability was calculated by plotting the flux against the applied pressure (Fig. 1b). It can be seen from Fig. 1b that flux and permeability decrease with the increase of the amount of formaldehyde associated with the active layer. It is also found that the flux through all membranes increases with rising pressure. The permeability of support, PF_1, PF_2 and PF_3 are found to be 1.565, 0.404, 0.232 and 4×10^{-2} L m^{-2} h^{-2} kPa^{-1}, respectively. However, there was no permeation through PF_4 and PF_5. The results indicated that the pore size and water absorbing property of the membrane significantly reduces with increase in amount of formaldehyde in the active layer.

MWCO study was conducted with PF_1, PF_2 and PF_3 using 10,000 mg L^{-1} of polyethylene glycol (MW: 1.5, 4, 6, 10 and 20 kDa) at 207 kPa and results are given in Fig. 1c. It was found that PF_1, PF_2 and PF_3 retained 90 % of PEG with the molecular weight of 15.55, 9.8 and 4.96 kDa, respectively.

The average pore radius of CM is estimated by Eq. (6) and it is in the order of 3.59 (PF_1) > 2.77 (PF_2) > 1.91 nm (PF_3). The reduction in pore size with the increase in the amount of formaldehyde might be due to the following reasons.

When PVA is crosslinked by formaldehyde, the available unbound –OH groups in the non-crystallization zones of polymer will interact with crosslinking agent as follows[31]:

$$\left[\begin{array}{c} CH{-}CH_2{-}CH{-}CH_2 \\ | \quad\quad\quad | \\ OH \quad\quad\ OH \end{array}\right] + HCHO \longrightarrow \left[\begin{array}{c} CH{-}CH_2{-}CH{-}CH_2 \\ | \quad\quad\quad | \\ O{-}CH_2{-}O \end{array}\right] + H_2O$$

The above reaction leads to intra-chain crosslinking which increases the polymeric crosslinking density and creates more compacted network structure. This reduces the chain mobility, tight fitting of chains, less swelling and tinny pores among the polymeric layer.[21]

Scanning electron microscope (SEM) analysis. SEM analysis was carried out to observe the morphological structure of ceramic support and different CMs. Fig. 2 shows the SEM images of the top surface of support and CMs synthesized by various compositions of PVA and formaldehyde. The morphological structure of ceramic support shows the micro and mesoporous nature of the membrane (Fig. 2a). SEM images depict that the surfaces of CMs get smoother as the amount of formaldehyde increases in polymeric solution.
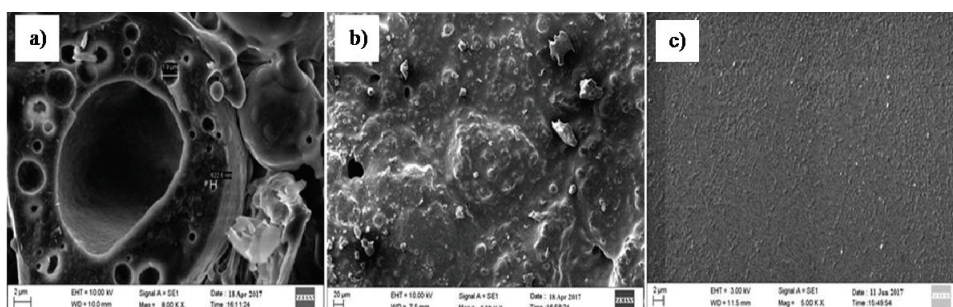

Fig. 2. SEM images of support and polymeric layers; a) ceramic support, b) pure PVA (PF$_0$) and c) crosslinked PVA (PF$_3$).

However, the PVA coating without crosslinking shows non-uniform surface of top layer (Fig. 2b). The increase in amount of crosslinking agent provides the tight fitting arrangement of particles in the membrane matrix which reduces the size of pores. Fig. 2c shows the smoother and pore free surface of PF$_3$ which is mainly due to the high compaction and rigidity at high crosslinking. Moreover, the increase in crosslinking resulted in the reduction of free volume and chain mobility of PVA and thus no permeation was observed through PF$_4$ and PF$_5$.[27]

Contact angle analysis. Contact angle analysis was carried out to understand the hydrophilicity and hydrophobicity nature of the synthesized CM. The contact angle between droplet and polymeric surface explains the wettability characteristic of layer. Fig. 3 shows the contact angle of different CMs with 13 µl water

droplet at ambient temperature. It was found that the contact angle between water droplet and active layer of CMs increased in order of $PF_0 < PF_1 < PF_2 < PF_3 < < PF_4 < PF_5$. The result indicates that the hydrophilic nature of CM decreases with the rise of the amount of cross linking agent due to the formation of the acetal group, which is hydrophobic in nature. The formation of the acetal group increases with the amount of crosslinking and that increase the hydrophobic group which reduces the hydrophilicity. The PF_0 has smallest contact angle of 32.44° with high hydrophilicity and wettability as compared to other CMs. PF_0 possesses highly rough as well as porous surface and that reduces while the amount of formaldehyde increases with PVA in other CMs.[31]
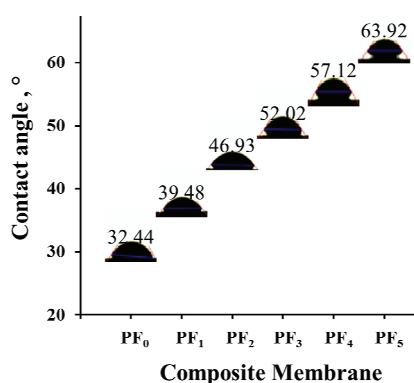

Fig. 3. Contact angle analysis of various active layers.

Phenol rejection

Selection of CM for phenol removal. Selection criteria of any membrane are mainly related to the percentage rejection of solute and permeation through the membrane. Fig. 4a shows time *versus* retention (bar chart) and time *versus* flux (line graph). Since the active layer of PF_0 is not stable on support, it was not further consider for phenol removal. Similarly, PF_4 and PF_5 were also not considered due to their impermeable nature. The phenol removal by PF_3 was found to be 71 % for 1 h time, which is higher than PF_2 (42 %) at a constant applied pressure (207 kPa), but phenol completely passed through PF_1. At equilibrium time (3 h), high flux was obtained for PF_1 (20.45 L m^{-2} h^{-1}) whereas for PF_2 (8.82 L m^{-2} h^{-1}) and PF_3 (2.77 L m^{-2} h^{-1}) flux decreased due to the decrease in pore size. The addition of crosslinking decreases the pore size and roughness of PF_2 and PF_3 membrane surface which reflects on solute penetration through PF_1 to PF_3.[31] Hence, PF_3 was considered for further studies due its high removal ability towards phenol.

Effect of feed concentration on phenol rejection and permeate flux. The feed phenol concentration was varied from 50–200 mg L^{-1} to observe the effect on rejection and flux through the PF_3 at 207 kPa. Fig. 4b represents time *versus*

rejection (bar chart) and flux (line graph) for various feed phenol concentration. It can be seen from the Fig. 4b that phenol rejection rises from 17.76 to 85 % with the increase in feed phenol concentration from 50-200 mg/l. The increase in rejection is attributed to the sorption of phenol by membrane material. To observe the phenol sorption capacity of CM, mass uptake by pure water was considered as zero. Mass uptake by CM in 50 mg L^{-1} phenol was found to be 3.32 wt. % which increased to 55.43 wt. % for 200 mg L^{-1}. This is approximately 17 times more than the initial concentration (50 mg L^{-1}). Hence the phenol sorption capacity of CM greatly affects the concentration of phenol on permeate side along with the sieving property of CM.[35] The flux decreased from 8.65 to 3.63 L m^{-2} h^{-1} when phenol concentration increased from 50 to 200 mg L^{-1}. This is due to the high concentration of phenol at the membrane-solution interface that may cause the concentration polarization which reduces the flux.
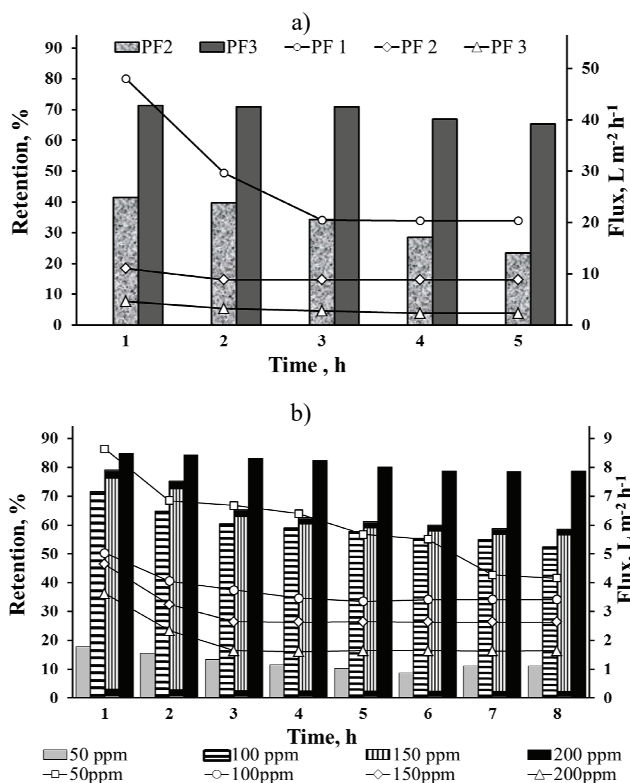

Fig. 4. Phenol rejection and flux profile for: a) different CMs; b) effect of feed phenol concentration with respect to time.

Effect of feed pH on phenol rejection and permeate flux. The effect of feed pH on separation performance and flux was examined using PF_3 with 100 mg L^{-1}

of feed phenol concentration at 207 kPa. Fig. 5a shows the effect of pH on phenol rejection efficiency and flux. It was observed that flux was unaffected by pH variation of feed. Phenol removal increases initially from 15 to 55 % when pH rises from 2 to 6, thereafter decreases to 11.4 % at pH 12.
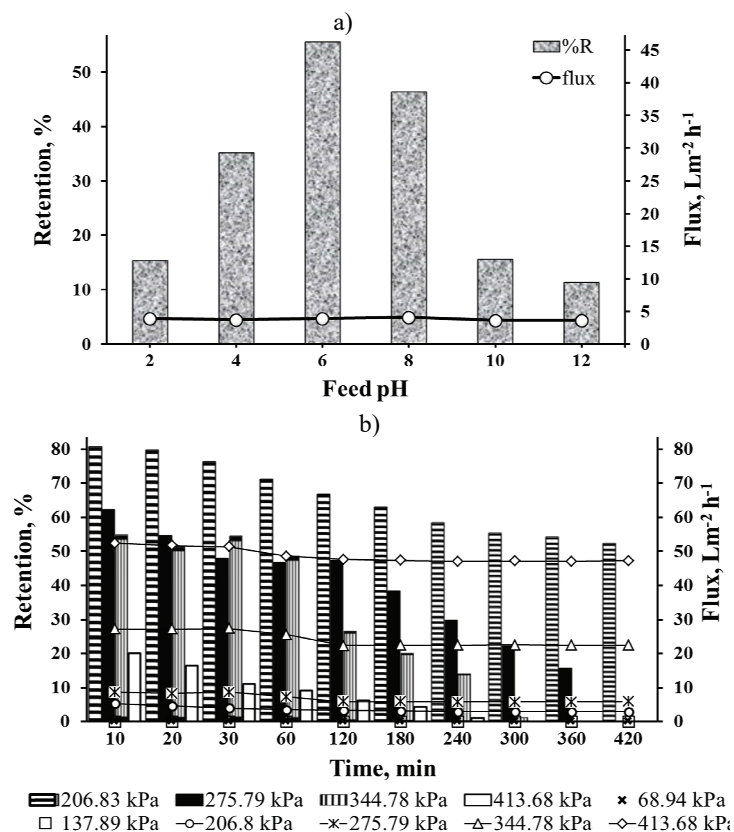

Fig. 5. Phenol rejection and flux profile for effect of: a) feed pH; b) pressure with respect to time.

Pressure dependency of separation performance. Fig. 5b shows the permeate flux and percentage rejection as a function of time with the various applied pressures. It was observed that the percentage removal decreases with increasing pressure.

The phenol removal increased from 1 to 58.4 % when pressure decreased from 414 to 207 kPa (Fig. 5b). This is due to the fact that at high pressure the smaller pores became permeable. Hence phenol permeated through the membrane and it resulted in higher phenol concentration in permeates side. However, at low pressure only wider pores allow the phenol permeation through the membrane and thus more phenol molecules were retained on CM which causes

high phenol removal.[12] Fig. 5b also represents the permeation flux of phenol at various pressures. The flux rises from 5.3 to 52.38 L m^{-2} h^{-1} with increase in pressure from 207 to 413 kPa.

Possible rejection mechanism of phenol

It is very important to find the mechanism of phenol removal by membrane which will eventually be a guide for the rational design of membrane separation process. Generally, phenol removal by membranes can be achieved by various mechanisms such as adsorption, molecular sieving and electrostatic repulsion or attraction. In this study, the possible phenol removal mechanism by PVA/ceramic composite membrane can be established by the following two steps: a) active/top film mechanism and b) substrate mechanism.

In the film mechanism, the hydrogen bonding sites of phenol forms the relatively strong hydrogen bonds with high electronegative oxygen molecules of crosslinked polymer (Fig. 6). Also, the physical adsorption of phenol in porous top layer occurs due to van der Waals force of attraction. But in the substrate mechanism, the chemical adsorption plays a vital role for phenol removal. In this work, substrate was fabricated by the fly ash and the fuller clay mixer. The fly ash and the fuller clay (major component: montmorillonite) consist of two major constituents such as alumina and silica (Fig. 6). In this, Si–O bond is ionic due to the large alteration in the electronegativity of oxygen and silicon, which adsorbs huge amounts of phenols, which are polar molecules. Besides, Al and Si metal
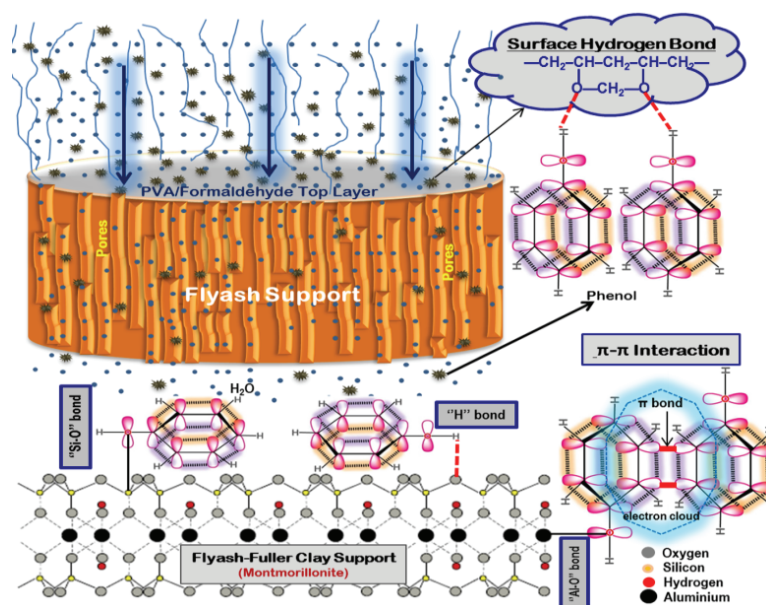

Fig. 6. Phenol separation mechanism by CM.

oxides produce metal hydroxide complexes at the solution interface leading to the development of a positive or negative charge on the surface which favours the phenol adsorption. Phenol might also be removed by composite membrane due to π-bond formation between two orbital of phenolic rings when they overlap (Fig. 6).

CONCLUSION

The CM prepared by the active layer of PVA crosslinked with varied quantity of formaldehyde on ceramic substrate was compared. The property of the active layer slightly changes with the increase in the amount of formaldehyde. The increase in formaldehyde proportion resulted in the decrease of the degrees of swelling, hydrophilicity, pore size, and permeability of CM. However, the stability of the active layer and rejection efficiency of CM increases. The average pore radius of CM determined by MWCO is in the range of 3.59 (PF_1) > 2.77 (PF_2) > 1.91 nm (PF_3) while PF_4 and PF_5 was found to be dense. CM with crosslinked PVA using 3 g of formaldehyde (PF_3) was found to be optimum for the separation of phenol/water mixture. The optimum conditions for operating parameters were found to be pH 6, 200 mg/l feed phenol concentration and 207 kPa operating pressure. The rejection of phenol increases with the feed phenol concentration, while the decreasing trend was obtained with the increasing pressure. The flux profile so obtained was decreasing with feed phenol concentration and increasing with pressure. The obtained result reveals that the simple glass coating method may be used to synthesize the CM, which could be applicable for phenol-water separation with good separation efficiency.

ИЗВОД
СИНТЕЗА КОМПОЗИТНЕ МЕМБРАНЕ УМРЕЖЕНИ PVA-КЕРАМИКА ЗА УКЛАЊАЊЕ ФЕНОЛА ИЗ ВОДЕНИХ РАСТВОРА

VANDANA GUPTA и JAYAPAL ANANDKUMAR

Department of Chemical Engineering, National Institute of Technology Raipur, Chhattisgarh-490210, India

У овом раду је синтетисана композитна мембрана за уклањање фенола из воде наношењем танког слоја формалдехидом умреженог поливинил-алкохола на керамички супстрат добијен од летећег пепела и глине. Танки филм је добијен коришћењем 10 % воденог раствора PVA са различитим количинама формалдехида (1–5 g на 10 g PVA). У циљу оптимизације мембране, примењене су различите методе карактеризације: одре-ђивање степена бубрења, хемијске стабилности, пермеабилности и молекулске масе материјала који се 90 %-ном ефикасношћу задржава на мембрани (MWCO), скенирајућа електронска микроскопија (SEM) и анализа контактног угла. Стабилност активног слоја се повећава са повећањем садржаја формалдехида, док се хидрофилност, степен бу-брења, флукс и величина пора смањују. Најмање поре (1,91 nm) у активном слоју су добијене када је PVA умрежен са 3 g формалдехида (узорак PF_3). Издвајање фенола из

воде је испитивано применом узорка PF$_3$ у циљу оптимизације процесних параметара, као што су концентрација напојног раствора, pH и притисак. Максимално уклањање фенола (85 %) је постигнуто при 207 kPa за концентрацију фенола од 200 mg L^{-1}. Висок степен уклањања је постигнут при pH 6,0 и са повишењем pH се смањивао. Степен уклањања фенола се смањивао са 80,6 на 19,8 % са повећањем притиска од 207 до 414 kPa, при чему се флукс повећавао са 5,3 на 52,38 L m^{-2} h^{-1}. Резултати су показали да је добијена композитна мембрана ефикасна за уклањање фенола из воде.

REFERENCES

1. B. Commoner, *J. Clean. Prod.* **5** (1997) 125 (https://doi.org/10.1016/S0959-6526(97)00011-5)
2. *Integrated risk information system.* https://archive.epa.gov/teach/web/pdf/benz_summary.pdf (accessed: 4.7.2016)
3. A. Mixa, C. Staudt, *Int. J. Cheme.* (2008) 1 (http://dx.doi.org/10.1155/2008/319392)
4. J. Sawai, N. Ito, T. Minami, M. Kikuchi, *J. Membr. Sci.* **252** (2005) 1 (https://doi.org/10.1016/j.memsci.2004.06.018)
5. M. Sagehashi, T. Nomura, H. Shishido, A. Sakoda, *Bioresour. Technol.* **98** (2007) 2018 (https://doi.org/10.1016/j.biortech.2006.08.022)
6. G. M. Zeng, K. Xu, J. H. Huang, X. Li, Y. Y. Fang, Y. H. Qu, *J. Membr. Sci.* **310** (2008) 149 (https://doi.org/10.1016/j.memsci.2007.10.046)
7. D. P. Zagklis, A. I. Vavouraki, M. E. Kornaros, C.A. Paraskeva, *J. Hazard. Mater.* **285** (2015) 69 (https://doi.org/10.1016/j.jhazmat.2014.11.038)
8. M. Hemmati, N. Nazari, A. Hemmati, S. Shirazian, *J. Ind. Eng. Chem.* **21** (2015) 1410 (https://doi.org/10.1016/j.jiec.2014.06.015)
9. A. Bodalo, E. Gomez, A. M. Hidalgo, M. Gomez, M. D. Murcia, I. Lopez, *Desalination* **245** (2009) 680 (https://doi.org/10.1016/j.desal.2009.02.037)
10. M. J. González-Muñoz, S. Luque, J. R. Álvarez, J. Coca, *J. Membr. Sci.* **213** (2003) 181 (https://doi.org/10.1016/S0376-7388(02)00526-4)
11. Y. Liu, M. Meng, J. Yao, Z. Da, Y. Feng, Y. Yan, C. Li, *Chem. Eng. J.* **286** (2016) 622 (https://doi.org/10.1016/j.cej.2015.10.063)
12. B. K. Nandi, R. Uppaluri, M. K. Purkait, *J. Membr. Sci.* **330** (2009) 246 (https://doi.org/10.1016/j.memsci.2008.12.071)
13. S. Jana, M. K. Purkait, K. Mohanty, *J. Membr. Sci.* **382** (2011) 243 (https://doi.org/10.1016/j.memsci.2011.08.011)
14. P. Mittal, S. Jana, K. Mohanty, *Desalination* **282** (2011) 54 (https://doi.org/10.1016/j.desal.2011.06.071)
15. I. Jedidi, S. Sai, S. Khmakem, N. Elloumi-ammar, A. Fourati, A. Charf, *Arabian J. Chem.* **2** (2009) 31 (https://doi.org/10.1016/j.arabjc.2009.07.006)
16. D. Vasanth, G. Pugazhenthi, R. Uppaluri, *Desalination* **320** (2013) 86 (https://doi.org/10.1016/j.desal.2013.04.018)
17. S. Y. Hu, Y. Zhang, D. Lawless, X. Feng, *J. Membr. Sci.* **417** (2012) 34 (https://doi.org/10.1016/j.memsci.2012.06.010)
18. T. Puspasari, N. Pradeep, K. V. Peinemann, *J. Membr. Sci.* **491** (2015) 132 (https://doi.org/10.1016/j.memsci.2015.05.002)
19. S. Y. Li, R. Srivastava, R. S. Parnas, *J. Membr. Sci.* **363** (2010) 287 (https://doi.org/10.1016/j.memsci.2010.07.042)
20. Y. Matsumoto, M. Sudoh, Y. Suzuki, *J. Membr. Sci.* **158** (1999) 55 (https://doi.org/10.1016/S0376-7388(99)00032-0)

21. B. Han, J. Li, C. Chen, C. Xu, S. R. Wickramasinghe, *Trans. ICheme, A* **81** (2003) 1385 (https://doi.org/10.1205/026387603771339609)
22. A. L. Ahmad, N. M. Yusuf, B. S. Ooi, *Desalination* **287** (2012) 35 (https://doi.org/10.1016/j.desal.2011.12.003)
23. B. Bolto, T. Tran, M. Hoang, Z. Xie, *Prog. Polym. Sci.* **34** (2009) 969 (https://doi.org/10.1016/j.progpolymsci.2009.05.003)
24. A. Hasimi, A. Stavropoulou, K. G. Papadokostaki, M. Sanopoulou, *Eur. Polym. J.* **44** (2008) 4098 (https://doi.org/10.1016/j.eurpolymj.2008.09.011)
25. A. Higuchi, T. D. Lijima, *Polymer* **26** (1985) 1833 (https://doi.org/10.1016/0032-3861(85)90011-4)
26. S. Jana, M. K. Purkait, K. Mohanty, *Desalin. Water Treat.* **37** (2012) 321 (http://dx.doi.org/10.1080/19443994.2012.661574)
27. R. Rudra, V. Kumar, P. P. Kundu, *RSC Adv.* **5** (2015) 83436 (https://doi.org/10.1039/c5ra16068e)
28. T. A. Peters, C. H. S. Poeth, N. E. Benes, H. C. W. M. Buijs, F. F. Vercauteren, J.T.F. Keurentjes, *J. Membr. Sci.* **276** (2006) 42 (https://doi.org/10.1016/j.memsci.2005.06.066)
29. G. Bourne, M. S. Buiser, T. V. Casey, S. Keenan, J. L. Lanphere, J. Li, E. P. Mckenna, Z. Minasian, D. Rao, US 7, 611, 542 B2 (2009)
30. K. Hunger, N. Schmeling, H. B. T. Jeazet, C. Janiak, C. Staudt, K. Kleinermanns, *Membranes* **2** (2012) 727 (https://doi.org/ 10.3390/membranes2040727)
31. Y. L. Lin, *J. Environ. Eng.* **139** (2013) 127 (https://doi.org/10.1061/(ASCE)EE.1943-7870.0000623)
32. R. Mukherjee, S. De, *J. Hazard. Mater.* **265** (2014) 8 (https://doi.org/10.1016/j.jhazmat.2013.11.012)
33. K. J. Kim, A. G. Fanen, R. Ben-Aim, M. G. Liu, G. Jonsson, I. C. Tessaro, A. P. Broek, D. Bargeman, *J. Membr. Sci.* **87** (1994) 35 (https://doi.org/10.1016/0376-7388(93)E0044-E)
34. *APHA 5530: Standard Method for Examination of Water and Wastewater*, American Public Health Association, Washington, DC, 2012
35. J. Han, J. Fu, R. B. Schoch, *Lab Chip.* **8** (2008) 23 (https://doi.org/ 10.1039/b714128a).